Investigation of AlGaN-Delta–GaN Based UV Photodiodes in a Metal–Semiconductor–Metal Configuration for Efficient and Fast Solar Blind UV Sensing

Solumtochukwu F. Nwabunwanne, Bryan Melanson, Jing Zhang, and William R. Donaldson

***Abstract*— Metal–semiconductor–metal (MSM) configuration UV photodiodes (PD's) were designed and fabricated on an AlGaN/GaN–based substrate for efficient and ultrafast UV detection. The purpose was to investigate the feasibility of obtaining efficient and ultrafast temporal response from these devices in the UV given the challenges associated with the formation of Schottky contacts on laterally oriented AlGaN/GaN thin films. Two sets of devices were implemented using Pt and Au as metal contacts with 5-μm finger width, 5-μm finger spacing, and a 50-μm × 50-μm active area. Spectral and voltage bias studies were done to establish the spectral profile and the effect of bias voltage on the responsivity of the detectors at 265 nm. The best vertical MSM PD's produced 0.6-A/W responsivity under 10-V bias voltage at 265 nm. Peak spectral responsivities were recorded as 1.35 A/W and 1.25 A/W at 240 nm for Pt and Au PD's respectively.**

***Index Terms*—AlGaN, GaN, efficient, spectral responsivity, PIN, MSM, UV, photodetector, vertically oriented, PD, Pt, Au.**

I. Introduction

Vertical epitaxial structures of aluminum-gallium-nitride (AlGaN) and gallium nitride (GaN) heterostructures, facilitate fast and efficient sensing of UV light in p-type–intrinsic–n-type (PIN) and avalanche configurations. Photodiodes (PD's) manufactured on AlGaN templates possess sharp cutoff edges, making them appropriate in setups that need multiple light sources in close proximity like in space exploration vehicles, plasma diagnostics, and target chambers for fusion experiments [1–4]. AlGaN heterostructures are attractive for UV sensing because they have tunable wide and direct-energy band gaps. GaN alloys can sense optical radiation spanning the entire UV spectrum. Spectral window selectivity is supported by simply changing the percentage of Al in the $Al_xGa_{1-x}N$ (x: 0 to 1) alloy [5–8]. Our group and others have reported that the metal–semiconductor–metal MSM configuration gives the fastest possible response for GaN/AlGaN-based PD's since, in this mode, the response time of the detector is carrier transit time limited. The small capacitance due to the narrow interdigitated fingers translates to ~1-ps resistor-capacitor (RC) time constant when terminated by a 50-Ω electrical load [9]. The ~1-ps time constant is usually ignored given that the carrier transit time is significantly greater than 1 ps in practice.

In this article, we report the successful design, implementation, and characterization of a novel class of AlGaN/GaN-based UV detectors. These new PD's harness the ultrafast capabilities of the MSM configuration and the robust quantum efficiency of p-i-n quantum wells (QW's). To the best of the authors' knowledge, MSM configured vertical epistacked GaN/AlGaN-based UV photodetectors have not been reported previously in literature. The objective of this research was to experimentally demonstrate the feasibility of obtaining ultrafast and efficient response from MSM PD's fabricated on p-i-n structured GaN/AlGaN templates under UV radiation. For this study, we employed the delta-GaN QW deep UV wafer configuration [10] shown in Fig. 1. Devices with different metal contacts yielded distinct temporal response parameters. An Au device produced a temporal response of 25.4-ps rise time with 415.8-ps pulse duration, while a Pt device recorded 16.6-ps rise time and 253.8-ps pulse width. Also, the responsivities of both Au and Pt devices had different peaks; Au PD peaked at 1.25 A/W [external quantum efficiency (EQE) = 646%] under 240-nm radiation while Pt PD had a maximum of 1.35 A/W (EQE = 684%) responsivity under 240 nm at 10-V bias. These >1 A/W responsivities indicate that the detectors were in photoconductive mode as a result of the multiplication of charge carriers within the QW, which degraded the response speed of the detectors.

Submitted 11 November 2022. Solumtochukwu F. Nwabunwanne is with Plasma and Ultrafast, Laser Science and Engineering Division, Laboratory for Laser Energetics, University of Rochester, Rochester, NY 14623 USA (e mail: solumtochukwu.nwabunwanne@ rochester.edu).

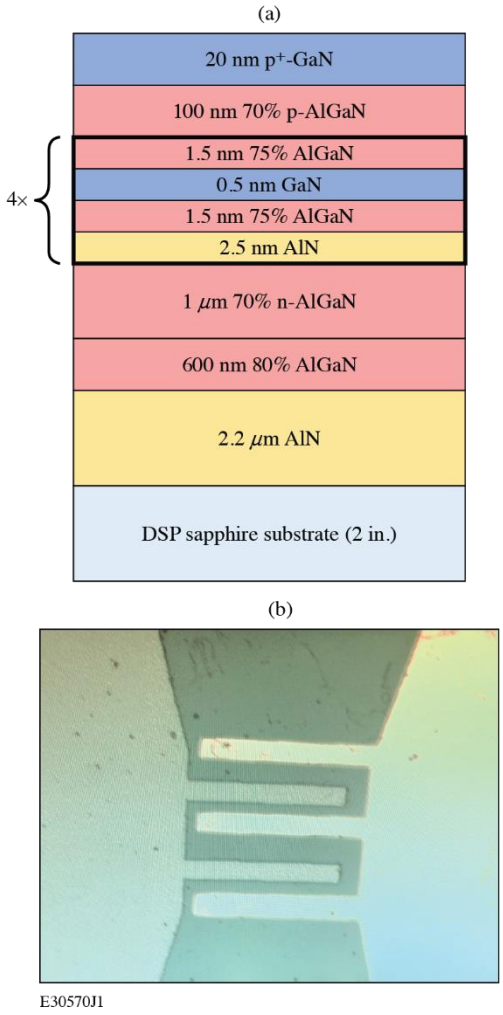

Fig. 1.(a) Epitaxial structure of p-i-n AlGaN/GaN thin films used to fabricate the vertical MSM UV PD's. (b) As-fabricated device showing the 50 μm × 50-μm active area, interdigitated contacts, and compensation pad.

II. Design and Manufacture of the Device

Given the challenges of formation of Schottky contacts and photoconductivity that are associated with laterally oriented AlGaN thin film MSM PD's, it was considered worthwhile to study the feasibility of using a vertically structured p-i-n AlGaN/GaN heterostructure on sapphire to obtain efficient and ultrafast UV photodetection. The customized AlGaN-delta-GaN QW wafer shown in Fig.1(a) was grown by metal organic chemical vapor deposition (MOCVD) [11]. The vertical epitaxial structure of these devices consists of a 2.2-μm AlN nucleation layer grown on a 50.8-mm-diam, 425-μm-thick sapphire wafer, followed by 600 nm of $Al_{0.8}Ga_{0.2}N$, 1 μm n-$Al_{0.7}Ga_{0.3}N$, and four QW pairs consisting of a 2.5-nm AlN barrier layer, a 1.5-nm $Al_{0.75}Ga_{0.25}N$ bottom sub-QW layer, a 0.50-nm GaN delta-layer, and a 1.5-nm $Al_{0.75}Ga_{0.25}N$ top sub-QW. The quantum wells are capped by a 100-nm-thick p-$Al_{0.7}Ga_{0.3}N$ layer and a 20-nm-thick p+-GaN contact layer. This particular configuration was optimized for a light-emitting diode application to enable us to share a foundry fabrication run with another project. Figure 2 shows the simulated photo-luminescence of this customized wafer with peak at 259 nm.

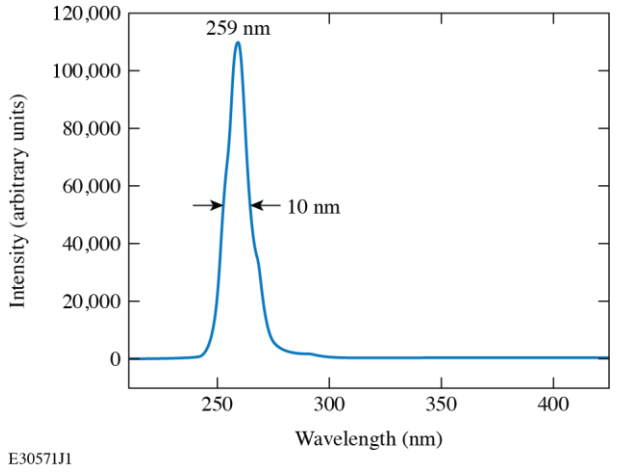

Fig. 2 Simulated photoluminescence of the epitaxial structure of the p-i-n AlGaN/GaN thin films (peaked at 259 nm with 10-nm FWHM) used to fabricate the vertical MSM UV PD's.

Fabrication of these PD's involved standard photolithography, physical vapor deposition, and plasma etching. Two categories of devices were designed, fabricated, and tested; one set of devices had Pt contacts and the other category had Au contacts.

The MSM structured devices on vertical oriented AlGaN/GaN heterostructure were fabricated at the Integrated Nanosystems Center (URnano) at the University of Rochester and Semiconductor & Microsystems Fabrication Laboratory of the Rochester Institute of Technology. Design files were created using the Clewin5 [12] application and then converted into laser draw files for execution by the laser writer. Positive KL6003 photoresist was employed for photolithography. Pt and Au were chosen as metal contacts to facilitate comparison with the previous MSM lateral detectors we reported previously [8,13]. Both metal contact types had 20 nm Ti as an adhesion layer with either 120 nm Pt or 120 nm Au as contact metals. Pt was evaporated via e-beam technology while Au was deposited using thermal evaporation. For n contact metallization, 300 nm was etched into the thin film to expose the n-AlGaN layer using 32 standard cubic centimeter per minute (SCCM) of Cl_2, 8 SCCM of BCl_3, and 5 SCCM of Ar at 75-W RF power and ran for 60 s. Figure 1(b) shows a top view of the device design that was fabricated, having a 50-μm × 50-μm active area, a total of five interdigitated electrodes of 5-μm finger width, and 5-μm finger spacing.

Prior to fabrication, x-ray diffraction measurements were conducted to ascertain the dislocation density of defects within the thin films since these material defects are linked with elevated dark currents and poor device performance. Five points were chosen at random within the 2-in wafer for the rocking curve investigation. The outcomes of the x-ray rocking curve measurements are depicted in Fig. 3. The dislocation density was recorded as 3.7119×10^7 cm^{-2}, which indicates that while the material is of good quality with respect to reported GaN/AlGaN material properties [14–16], there are significant numbers of defect sites within the thin films. It is estimated that the number of defects within each detector is approximately 925 given that the detector's active area is 50 μm × 50 μm.

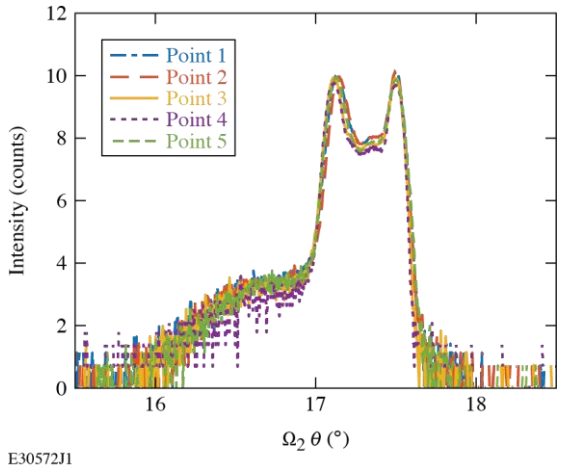

Fig. 3. p-i-n AlGaN/GaN thin film x-ray rocking curves along 002 direction at five different points on the thin film.

The current-voltage (IV) characteristics of one of the MSM-configured p-i-n AlGaN/GaN-based UV detectors under dark condition is illustrated in Fig. 4. It is evident that the quantum barrier is overcome at a bias voltage of 7 V, at which point the diodes begins to conduct. Peak current in forward bias mode is 8.2 μA at 20 V and 9.88 μA in reverse bias mode at -20 V. Also shown on Fig. 4 is the difference between the forward and reverse bias current with respect to the bias voltage. It is apparent that the asymmetry begins when the detector switched on.

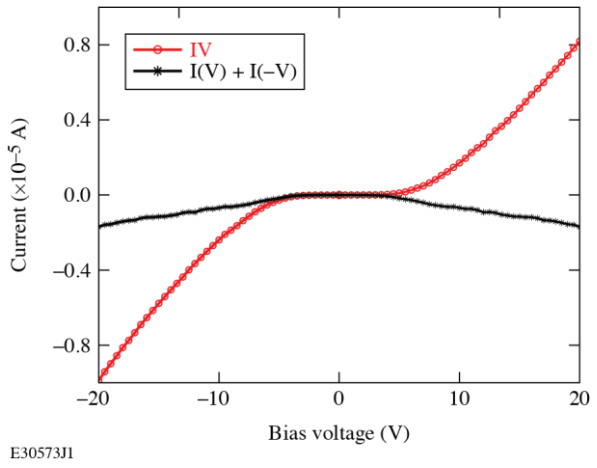

Fig. 4. IV curve of Pt RA MSM configured p-i-n AlGaN/GaN UV PD under dark condition, the asymmetry in the IV is shown by the black curve.

This ~17 % difference between forward and reverse bias current of the device suggests that Schottky contact may not be the reason for the diode behavior of the device, but the quantum well is. This is because current is confined within the quantum wells, such that Schottky contacts only serve to provide electrical connection with the external circuitry for biasing the device and signal transmission. Also, Schottky didoes require that two metal/semiconductor junctions be arranged back to back, so that the depletion regions overlap, to provide expected diode rectification, in these devices, however, there is a vertical separation between the contacts because they were grown on distinct semiconductor layers (n and p regions). This implies that the contacts, via the interdigitated fingers, function to regulate the carrier transit time by creating the shortest, practically possible electrical path to the external measurement system. Furthermore, MSM PD's with Schottky contacts exhibit symmetry in their IV curves [8] while some discrepancies may exist in p-i-n diodes due to the complex carrier dynamics with respect to the electric field within the quantum well [17,18]. The variation in the amplitude of the dark current with respect to the bias voltage is attributable to the asymmetric gain in the quantum well multiplication of carriers driven by the polarity of the electric field. Electrons and holes possess different mobilities; therefore, they travel at different speeds as a function of the electric field. At elevated electric fields (as is within these detectors), carrier collisions create additional charge carriers via impact ionization which is the physics behind the gain. The multiplication factor (M) in a two carrier system is given by Eq. (1) [19]:

$$M = \frac{a_e - a_h}{a_e * e^{-(a_e - a_h)*w} - a_h} \quad (1)$$

where w is width of the intrinsic region, and a_e and a_h are the electron and hole ionization coefficients, respectively. On the other hand, if the multiplication is only due to the electron, then ionization ratio (k) specifies the achieved gain and $k = (\propto_e)/(\propto_h)$ [19].

III. Investigations

The same external broadband coupling circuit and experimental setup used to characterize the ultrafast temporal response and external quantum efficiency profiles of the laterally oriented MSM AlGaN PD's given in [13] was employed to test the vertically oriented MSM AlGaN/GaN PD's for ultrafast UV photosensing. Figure 5 shows the impulse response functions of Au and Pt MSM configured p-i-n AlGaN-Delta-GaN devices under 20-V bias.

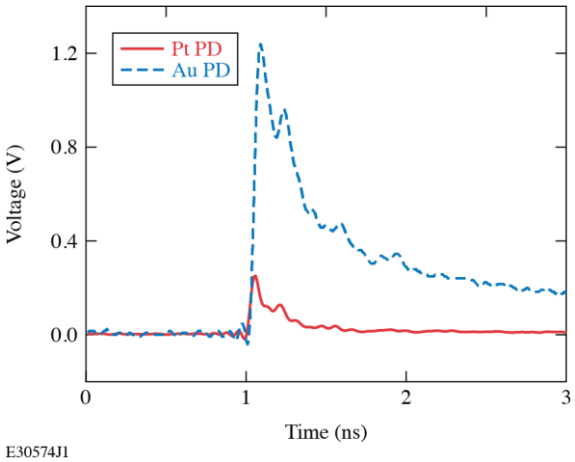

Fig. 5. Au and Pt devices with 25.4-ps, 16.6-ps rise time and 415.8-ps, 253.8-ps pulse width, respectively.

The two devices under test were excited by 265-nm, 30-fs short UV pulses and yielded 25.4-ps, 16.6-ps rise time and 415.8-ps, 253.8-ps full width half maximum (FWHM), respectively. For the Au device there is a considerable tail that extends beyond 2 ns after excitation.

There is a second peak in both response functions of the Au and Pt MSM-configured p-i-n AlGaN-Delta-GaN devices that occur ~200 ps after the primary photoexcitation peak. The presence of these peaks broadened the effective pulse width (FWHM) of the device even though the individual temporal features remained narrow. These secondary peaks in the response functions are likely due to the presence of the 0.5-nm delta GaN layers within the quantum well. Being that this vertical epi structure was primarily set up for light emitting diodes (LED's) [10], the GaN layer was introduced to enhance the electron-hole wave-function overlap in the quantum well. In the absence of the GaN layer, electron hole wave functions will drift to opposite sides of the AlGaN QW because of the material's internal polarization fields. This will drastically reduce the radiative recombination rate of any LED grown on this epitaxial structure, consequently reducing its efficiency. Therefore, adding the GaN layers will increase the recombination of electron-hole pairs in the AlGaN QW's. Additional carriers can be generated by deep UV excitons [20], produced in the AlGaN sub-QW layers, which recombine and emit photons before being removed from the QW. The longer-wavelength photons are then reabsorbed by the 2-nm GaN layer. These generated carriers are later removed, leading to the secondary peak in the response function. These reabsorbed carriers take approximately 200 ps to acquire sufficient energy from the present high electric field to be re-emitted from the quantum well [21,22]. Hence, eliminating the very thin GaN layer may remove the secondary peak at the cost of reducing the internal quantum efficiency of the detector.

IV. Spectral Voltage Studies Outcomes and Discussions

To determine the effect of bias voltage on the temporal response profile of the MSM p-i-n PD's, rise time and pulse duration were studied as functions of bias voltage from 0 to 20 V under 262-nm illumination. The outcome of this investigation is shown in Fig. 6(a). We see that from 0 to ~2.5 V, there were no significant data since the QW barrier had yet to be overcome. This implies that the carriers' transit time from in the QW at this range is greater than the recombination time of the carriers in the QW. Then between 3 V to 20 V, both rise time and pulse duration appeared to have a constant behavior with mean values of 34 ps and 300 ps, respectively. Figure 6(b) displays the rise time and pulse duration as functions of the incident light's wavelength.

While the rise time appeared to be unaffected by wavelength changes, the pulse duration showed significant variations. This further supports the hypothesis that the secondary peak in the response is because of the 2-nm GaN layer in the intrinsic sub-QW as the pulse duration of the response profile varied with wavelength in Fig. 6(b).

A Lambda 950 photo spectrometer was employed to measure the transmission profile of the p-i-n AlGaN/GaN thin film used to fabricate the devices under review. The data from this measurement listed in Fig. 7 show that cutoff edge of the device is 268 nm (4.64 eV). The additional 20% transmission loss at 300 nm is attributable to variations in the refractive index [$n(\lambda)$] of AlGaN/GaN with respect to input light's wavelength as described by Engelbrecht [23].

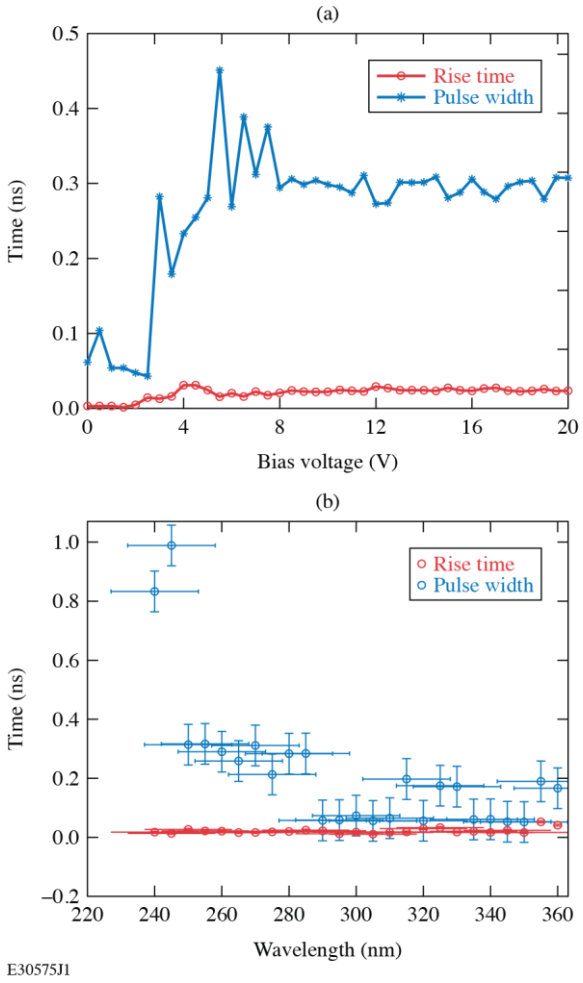

Fig. 6. Typical MSM configured p-i-n AlGaN/GaN PD rise time and pulse duration as functions of (a) bias voltage bias under 262-nm illumination. (b) Optical excitation wavelength under 10-V bias.

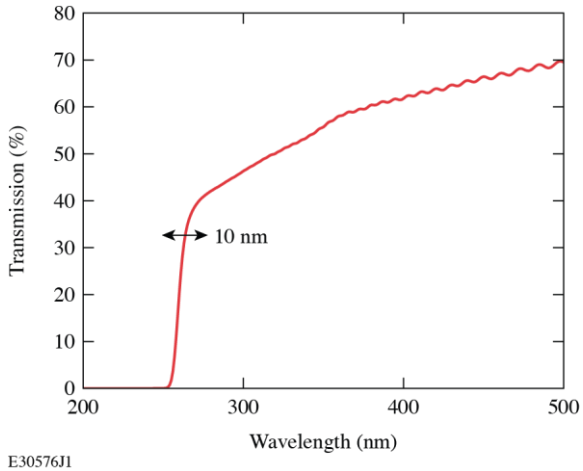

Fig. 7. Transmission profile of p-i-n AlGaN/GaN thin film with 10 nm FWHM from PL data highlighted by the blue arrow.

The responsivity versus wavelength measurements of Au and Pt devices shown in Fig. 8(b) suggest that there are likely two devices within each PD. This is due to the dual materials used in the absorption layer of the QW. The ~12-nm-thick AlGaN layers in the QW with ~75 % Al are responsible for the first cutoff edge seen at 268 nm, while the ~2-nm-thick GaN

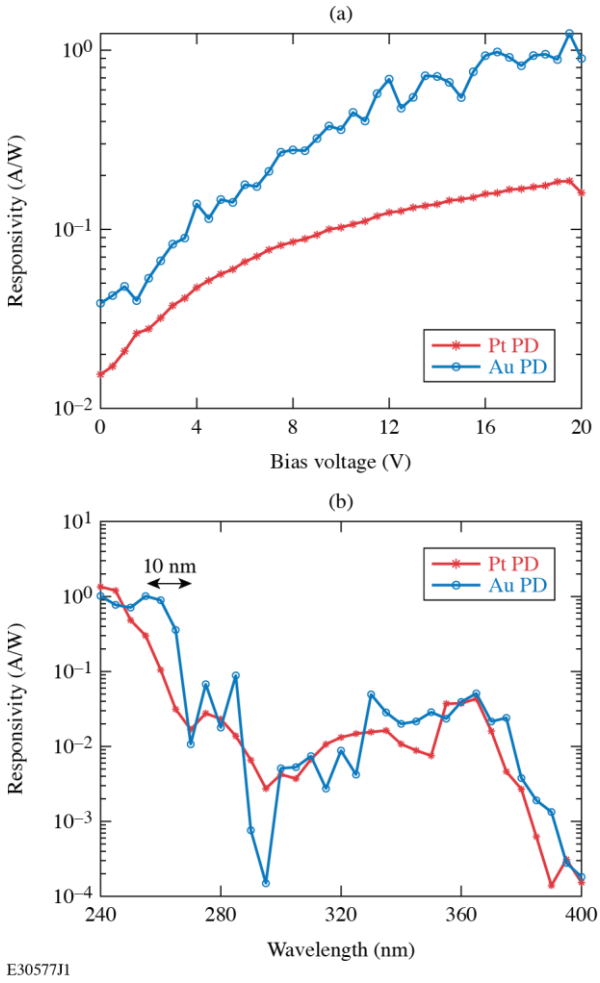

Fig. 8. Responsivity as a function of (a) bias voltage at 262-nm illumination and (b) wavelength under 10 V for Au and Pt devices. The blue arrow indicates the 10 nm FWHM.

layers account for the responsivities from 310 nm to 380 nm in Fig. 8(b). The variations in the responsivities of both Au and Pt devices are likely a result of nonuniformity of material properties within the semiconductor thin films. The differences may also be attributed to the higher work function of Pt that modified the device functional condition at the heterojunction of the metal and semiconductor. This implies that $E_g > h\nu > q\phi_{metal}$ and $V < V_B$ and internal photoemission is operational at different levels within both Au and Pt devices [8,24].

$$R = \frac{I_{ph}}{P} \tag{2}$$

where I_{ph} (photocurrent) = illumination current (dark current in amperes) and P is the incident optical power on the detector in watts.

Equation (2) was used to calculate the responsivity of Au and Pt MSM configured p-i-n AlGaN/GaN detectors versus bias voltage and wavelength, with the outcomes plotted in Fig. 8(a) and (b), respectively. From Fig. 8(a), both devices exhibited their peak responsivities at 19.5 V with Pt PD having 0.2 A/W and Au PD showing 1.2 A/W at 8.19-μA dark current. The linear relation between responsivity and bias suggest that the device has yet to attain saturation. The spectral responsivity profiles of both devices are shown in Fig. 8(b) indicating the 10-nm cutoff edge shown in Figs. 2 and 7. Here the Pt device exhibited a maximum responsivity of 1.35 A/W at 240 nm with a sharp cutoff at 260 nm. The Au device on the other hand peaked with 1.25 A/W at 240 nm with a cutoff at 265 nm. This 5-nm difference in the cutoff edges of both devices maybe attributable to the ~0.46-eV difference in Pt and Au Schottky barrier heights.

The data in Fig. 9 is from the Au p-i-n AlGaN/GaN device at 351-nm UV illumination under 20-V bias and a conventional MSM AlGaN PD, which was illuminated by a 262-nm UV light yielding 32-ps rise time and 62 ps FWHM. At 351 nm, the AlGaN layers of the QW in the Au p-i-n AlGaN/GaN device should be transparent and non-absorbing; the absorption will occur only in the GaN layers. The carrier recycling mechanism discussed above can still operate. These data suggest that it possible to obtain ultrafast response using MSM configuration on a p-i-n AlGaN/GaN structure, but it will require optimization of the QW design to yield a single peak. This will be the subject of a future publication. Hence, obtaining a single peak from the next-generation p-i-n AlGaN/GaN devices should yield a response time that is approximately equal to the pulse duration as the first peak of Au p-i-n AlGaN/GaN device in Fig. 9, which is 75 ps. For comparison the conventional MSM PD's response time is 62 ps. Therefore, the p-i-n structure appears to have only slightly degraded the pulse width, but it should remain viable for many of the target applications.

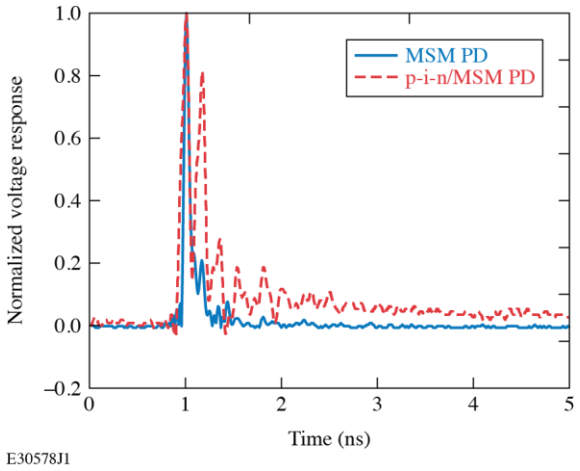

Fig. 9. Temporal response of Au p-i-n AlGaN/GaN device at 351-nm UV excitation under 20-V bias with 39.2-ps rise time, 121.7-ps pulse duration, and a conventional lateral MSM PD under 262-nm illumination and 20-V bias, with 32-ps rise time, 62-ps pulse duration.

V. Conclusion

In summary, we have successfully demonstrated the feasibility of obtaining efficient and ultrafast UV photodetection with MSM configured vertically oriented AlGaN/GaN-based UV PD's. Voltage studies showed that the devices had a linear responsivity profile with bias voltage from 3.5 V to 15.5 V for an Au device, while the Pt device showed linearity from 3.5 V to 19.5 V. This implies that saturation was imminent in the Au device from 15.5 V. The spectral responsivity of Pt and Au devices are comparable at 1.35 A/W at 240 nm with a sharp cutoff at 260 nm and 1.25 A/W at 240

nm with a cutoff at 265 nm, respectively. Finally, the temporal response of both devices showed that Pt devices had better temporal characteristics with 16.6-ps rise time and 253.8-ps pulse duration, while Au devices had a 25.4-ps rise time and 415.8-ps pulse width due to its long decay tail. These interesting outcomes will provide an alternative path to Schottky contact formation challenges in achieving efficient and ultrafast photosensing in the UV region. It is intended that these novel devices will forge a paradigm shift in the way AlGaN/GaN-based MSM PD's are designed for the high-energy-density physics and the plasma diagnostics community.

ACKNOWLEDGMENT

This material is based upon work supported by the Department of Energy National Nuclear Security administration under Award Number DE-NA0003856, the University of Rochester, and the New York State Energy Research and Development Authority. Additional support was supplied by a DOE SBIR grant to Sydor Technologies, of which the University of Rochester Laboratory for Laser Energetics is a Subcontractor.

This report was prepared as an account of work sponsored by an agency of the U.S. Government. Neither the U.S. Government nor any agency thereof, nor any of their employees, makes any warranty, express or implied, or assumes any legal liability or responsibility for the accuracy, completeness, or usefulness of any information, apparatus, product, or process disclosed, or represents that its use would not infringe privately owned rights. Reference herein to any specific commercial product, process, or service by trade name, trademark, manufacturer, or otherwise does not necessarily constitute or imply its endorsement, recommendation, or favoring by the U.S. Government or any agency thereof. The views and opinions of authors expressed herein do not necessarily state or reflect those of the U.S. Government or any agency thereof.

REFERENCES

1. R. Young, C. C. Kuranz, D. H. Froula, J. Ross, and S. Klein, "Observation of stagnation in counter-streaming laser-created plasmas with optical Thomson scattering," *Bull. Am. Phys. Soc.*, vol. 63, no. 11, p. BAPS.2018.DPP.GO2014.2011, Jan. 2018.
2. A. M. Hansen *et al.*, "Cross-beam energy transfer platform development on omega," *Bull. Am. Phys. Soc.*, vol. 63, no. 11, p. BAPS.2018.DPP.CO2014.2017, Jan. 2018.
3. A. M. Saunders *et al.*, "Characterizing plasma conditions in radiatively heated solid-density samples with x-ray Thomson scattering," *Phys. Rev. E*, vol. 98, no. 6, Art. no. 063206, Dec 2018, doi: 10.1103/PhysRevE.98.063206.
4. B. E. Kruschwitz *et al.*, "Tunable UV upgrade on OMEGA EP," *Proc. SPIE*, vol. 10898, Art. no. 1089804, Mar 2019, doi: 10.1117/12.2505419.
5. E. Monroy, F. Calle, E. Muñoz, and F. Omnès, "AlGaN metal–semiconductor–metal photodiodes," *Appl. Phys. Lett.*, vol. 74, no. 22, pp. 3401–3403, May. 1999, doi: 10.1063/1.123358.
6. Q. Lyu, H. Jiang, and K. M. Lau, "Monolithic integration of ultraviolet light emitting diodes and photodetectors on a p-GaN/AlGaN/GaN/Si platform," *Opt. Express*, vol. 29, no. 6, pp. 8358–8364, Mar. 2021, doi: 10.1364/OE.418843.
7. M. Gökkavas, S. Butun, T. Tut, N. Biyikli, and E. Ozbay, "AlGaN-based high-performance metal–semiconductor–metal photodetectors," *Photonics Nanostructures: Fundam. Appl.*, vol. 5, no. 2, pp. 53–62, Oct. 2007, doi: 10.1016/j.photonics.2007.06.002.
8. S. F. Nwabunwanne and W. R. Donaldson, "Boosting the external quantum efficiency of AlGaN-based metal–semiconductor–metal ultraviolet photodiodes by electrode geometry variation," *IEEE J. Quantum Electron.*, vol. 57, no. 6, Art. no. 4000608, Dec. 2021, doi: 10.1109/JQE.2021.3117953.
9. Y. Zhao and W. R. Donaldson, "Ultrafast uv AlGaN metal–semiconductor–metal photodetector with a response time below 25 ps," *IEEE J. Quantum Electron.*, vol. 56, no. 3, Art. no. 4000607, Jun. 2020, doi: 10.1109/JQE.2020.2981043.
10. C. Liu, B. Melanson, and J. Zhang, "AlGaN-delta-GaN quantum well for DUV LEDs," *Photonics*, vol. 7, no. 4, Art. no. 87, Oct. 2020, doi: 10.3390/photonics7040087.
11. Precision Micro-Optics, "Gallium nitride (GaN) wafers," Accessed October 18, 2022, https://pmoptics.com/gallium_nitride.html.
12. "Clewin 5, regular 5-seat commercial license–wieweb software," Accessed 20 April 2021, https://wieweb.com/site/product/clewin-5-regular-5-seat-commercial-license/.
13. S. Nwabunwanne and W. Donaldson, "Interdigitated electrode geometry variation and external quantum efficiency of GaN/AlGaN-based metal–semiconductor–metal UV photodetectors," *Proc. SPIE*, vol. 12001, Art. no. 120010F, Mar. 2022, doi: 10.1117/12.2608355.
14. R. Gaska *et al.*, "Electron transport in AlGaN–GaN heterostructures grown on 6h–SiC substrates," *Appl. Phys. Lett.*, vol. 72, no. 6, pp. 707–709, Feb. 1998, doi: 10.1063/1.120852.
15. A. Chatterjee *et al.*, "Role of threading dislocations and point defects in the performance of GaN-based metal–semiconductor–metal ultraviolet photodetectors," *Superlattices Microstruct.*, vol. 148, Art. no. 106733, Dec. 2020, doi: 10.1016/j.spmi.2020.106733.
16. Y. Zhao and W. R. Donaldson, "Systematic study on aluminum composition nonuniformity in aluminum gallium nitride metal–semiconductor–metal photodetectors," *IEEE Trans. Electron Devices*, vol. 65, no. 10, pp. 4441–4447, Oct. 2018, doi: 10.1109/TED.2018.2862901.
17. Z. Zhang *et al.*, "AlGaN solar-blind p-i-n-i-n APDs employing a charge layer with modulated doping and bandgap," presented at *Asia Communications and Photonics Conference (ACPC) 2019*, OSA Technical Digest Chengdu: Optica Publishing Group, 2019, p. M4A.303, doi: 10.1364/ACPC.2019.M4A.303.
18. N. Biyikli, I. Kimukin, O. Aytur, and E. Ozbay, "Solar-blind AlGaN-based p-i-n photodiodes with low dark current and high detectivity," *IEEE Photon. Technol. Lett.*, vol. 16, no. 7, pp. 1718–1720, Jul. 2004, doi: 10.1109/LPT.2004.829526.
19. L. Chrostowski and M. Hochberg, *Silicon photonics design: From devices to systems*, 1st ed., Cambridge University Press, 2015, pp 259–294.
20. J. Yin *et al.*, "Surface plasmon enhanced hot exciton emission in deep UV-emitting AlGaN multiple quantum wells," *Adv. Opt. Mater.*, vol. 2, no. 5, pp. 451–458, Mar. 2014, doi: 10.1002.adom.201300463.
21. I. Sayed and S. M. Bedair, "Quantum well solar cells: Principles, recent progress, and potential," *IEEE J. Photovolt.*, vol. 9, no. 2, pp. 402–423, Mar. 2019, doi: 10.1109/JPHOTOV.2019.2892079.
22. J. A. Brum, T. Weil, J. Nagle, and B. Vinter, "Calculation of carrier capture time of a quantum well in graded-index separate-confinement heterostructures," *Phys. Rev. B*, vol. 34, no. 4, pp. 2381–2384, Aug. 1986, doi: 10.1103/PhysRevB.34.2381.
23. J. A. A. Engelbrecht, B. Sephton, E. Minnaar, and M. C. Wagener, "An alternative method to determine the refractive index of $Al_xGa_{1-x}N$," *Physica B Condens. Matter*, vol. 480, pp. 181–185, Jan 2016, doi: 10.1016/j.physb.2015.08.047.
24. S. M. Sze, *Semiconductor devices: Physics and technology*, 3rd ed., Hoboken, NJ: Wiley, 2012, pp. 29–40 and 76–78.

Solumtochukwu F. Nwabunwanne received both the B.Eng. degree in 2007 and the M.Eng. degree in 2013 in Electronic Engineering from the Department of Electronic Engineering, University of Nigeria, Nsukka, Nigeria. He received the M.S. degree in Electrical Engineering from the University of Rochester in 2019, where he is currently studying for the Ph.D. degree in Electrical Engineering. He is presently conducting research on ultrafast AlGaN-based UV photodetectors at the Laboratory for Laser Energetics.

Bryan Melanson received his B.S. degree in Materials Science and Engineering with a focus in Nanotechnology and Nanoengineering in 2018 from the University of Washington, Seattle, USA. He joined Dr. Jing Zhang's research group at the Rochester Institute of Technology as a Ph.D. candidate in 2018 and is currently conducting research on deep-ultraviolet light emitting diodes and µLED displays with a focus on improving the light extraction efficiency of these devices.

Jing Zhang is currently the Kate Gleason Associate Professor in the Department of Electrical and Microelectronic Engineering at Rochester Institute of Technology. She obtained B.S. degree in Electronic Science and Technology from Huazhong University of Science and Technology (2009), and Ph.D. degree in Electrical Engineering from Lehigh University (2013). Dr. Zhang's research focuses on developing highly efficient III-Nitride and GaO semiconductor based photonic, optoelectronic, and electronic devices. Her research group is working on the development of novel quantum well active regions and substrates for enabling high-performance ultraviolet (UV) and visible LEDs/ lasers, as well as engineering of advanced device concepts for nanoelectronics. Dr. Zhang has published more than 40 refereed journal papers and 70 conference proceedings including invited talks. She is a recipient of Texas Instruments/Douglass Harvey Faculty Development Award, and National Science Foundation (NSF) CAREER Award.

William R. Donaldson (Life Member, IEEE) received the B.S. degree (Hons.) in physics and mathematics from Carnegie Mellon University in 1976 and the Ph.D. degree from the Electrical Engineering Department, Cornell University, in 1984 on the use of organic crystals for an optical parametric oscillator. After graduating in 1984, he joined the Laboratory for Laser Energetics, University of Rochester, as a Research Associate. In 1986, he was promoted to Staff Scientist. In 2009, he was appointed as a professor of Electrical and Computer Engineering with the ECE Department, University of Rochester. His research interests have included the physics of photoconductive switches, streak-camera development, optical response of high-temperature superconductors, optical semiconductor diagnostics, and the florescence of biological molecules. He holds five patents and has published numerous scientific articles. He is a member of the American Physical Society and the Optical Society of America.